IEEE Access
Multidisciplinary ⋮ Rapid Review ⋮ Open Access Journal

Received May 17, 2021, accepted June 30, 2021, date of publication July 12, 2021, date of current version July 30, 2021.

Digital Object Identifier 10.1109/ACCESS.2021.3096419

Synthesis of Planar and Conformal Single-Layered Double-Sided Parallel-Cross Dipole FSS Based on Closed-Form Expression

YASSINE ZOUAOUI[1], LARBI TALBI[1], (Senior Member, IEEE), KHELIFA HETTAK[1], (Senior Member, IEEE), AND NARESH K. DARIMIREDDY[2], (Senior Member, IEEE)

[1]Department of Computer Science Engineering, University of Quebec in Outaouais (UQO), Gatineau, QC J8Y 3G5, Canada
[2]Department of Mathematics, Computer Science and Engineering, University of Quebec at Rimouski (UQAR), Rimouski, QC G5L 3A1, Canada

Corresponding author: Yassine Zouaoui (zouy01@uqo.ca)

ABSTRACT A simple synthesis method for ultra-thin double-sided cross-dipole-based Frequency Selective Surfaces (FSS) is presented in this paper. The presented technique is used to design a flexible band-stop FSS for Electromagnetic Interference (EMI) shielding applications operating at 10 GHz. An Equivalent Circuit (EC) model in combination with closed-form expression is used to synthesize and validate the response of the proposed element. In addition, a parametric study of the proposed FSS aiming to optimize the bandwidth has been presented. The proposed FSS holds similar responses for TE and TM mode of polarization at normal incidence. Further, the conformal behavior of the proposed FSS in comparison with planar FSS is presented and evaluated. The proposed FSS is validated with the full-wave EM solver for simulation and a prototype is fabricated. The size of the proposed unit cell is $0.4\lambda_0 \times 0.4\lambda_0$, where λ_0 is the free space wavelength at the desired the resonant frequency. In addition, the fractional bandwidth for TE and TM modes is 10.42% at normal incidence. The measured results of a proposed FSS are presented and validated in comparison with the simulations with good agreement.

INDEX TERMS Frequency selective surfaces, equivalent circuit model, bandwidth, conformal elements.

I. INTRODUCTION

Recently, a new concept of periodic structures is used to meet the rapid development of communication technology in terms of high data rates and system capacity. The idea revolves around the deployment of periodic structures into the building walls to make the propagation environment more favorable [1]–[4]. Among these periodic structures, FSS is a prominent structure used to isolate interference with adjacent wireless systems and enhance wireless security. Moreover, several numerical techniques have been proposed to analyze FSS. These techniques include full-wave analysis [5], iterative approach [6], and an equivalent circuit model [7]–[10]. As the electromagnetic performance of the FSS can be expressed by the inductive and capacitive behavior, the equivalent circuit model is the most widely used technique due to its simplicity. The analysis of FSS is essentially a method based on geometric parameters like the period of the unit cell (p), metal length (l), metal width, and the gap between the adjacent strips (g). In these techniques, the knowledge of the physical parameters is vital for accurate design.

On the other hand, to find these parameters for given filtering properties, a few synthesis methods are presented in the literature, especially for double-sided parallel-cross-dipoles-based FSS. In this regard, this paper proposes a straightforward technique for synthesizing a flexible double-sided parallel cross-dipoles-based FSS for a particular frequency band and provides the required size for the double-sided parallel cross-dipoles topology. Besides, producing a specific bandwidth is another degree of freedom relevant to the proposed synthesis technique and is different from the techniques reported in the open literature. The double-sided parallel cross-dipoles-based FSS in the article is a deformation of the Jerusalem cross-slot [11]. However, the proposed closed-form equations in this paper deal with FSS synthesis. The proposed synthesis method in this paper allowing the prediction of the physical parameters of the unit cell for Double-Sided Parallel-Cross Dipole FSS operating at 10 GHz and for an

The associate editor coordinating the review of this manuscript and approving it for publication was Flavia Grassi.

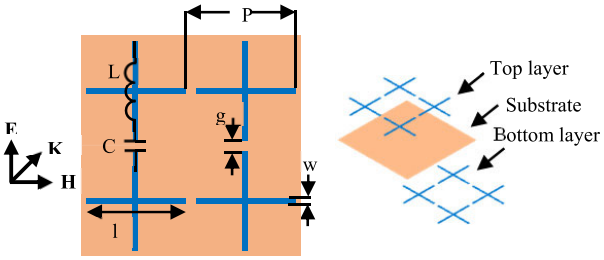

(a) Top and bottom view of the double-sided parallel cross-dipole array (FSS)

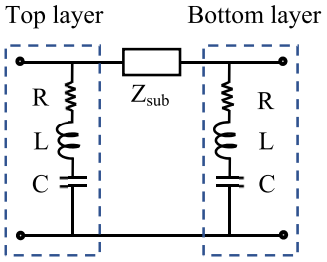

(b) Transmission Line Model

FIGURE 1. Double-sided parallel cross dipoles FSS structure and its equivalent circuit model.

arbitrary value of quality factor $\boldsymbol{Q} = \mathbf{7.5}$. The proposed FSS has the same frequency response for TE and TM polarizations with a fractional bandwidth of 10.42% at normal incidence. In addition, the structure presents a high level of shielding performance for both polarizations.

The Section II of the manuscript explains the theory of operation of double-sided parallel cross dipoles-based FSS. In Section III, the result obtained by the analytical solution is compared with the numerical simulation. Section IV explores the bandwidth control technique of double-sided parallel cross-dipoles. In Section V, the band-stop principle of double-sided parallel cross-dipoles FSS design at 10 GHz has been explored. Finally, the work is concluded in Section VI.

II. THEORETICAL APPROACH

According to Marcuvitz [12], the electromagnetic behavior of the metal strip lines is represented by the polarization of the wave. The parallel strips to the electric field are equivalent to an inductive element, and the perpendicular strips to the electric field correspond to a capacitive element, as presented in Fig. 1(a). The proposed double-sided parallel cross-dipoles-based FSS can be described by the equivalent circuit model shown in Fig. 1(b).

The equivalent circuit model of the proposed FSS is shown in Fig. 1(b), represents a band-stop filter. With this circuit, a double-sided parallel cross dipoles FSS can be synthesized to control the reflection level of the signal and the bandwidth enhancement. Therefore, by specifying the operating frequency $\left(f_0 = 1/2\pi\sqrt{LC}\right)$ [13] and the approximate quality factor of the overall circuit $(Q_1 + Q_2)/2$, where $\left(Q_1 = Q_2 = \sqrt{L}/R\sqrt{C}\right)$ [14], all the circuit parameters can be determined. The first step in the proposed synthesis procedure is to obtain the parameters of the equivalent circuit model presented in Fig. 1(b). The series RLC resonator is implemented with the periodic arrangement of the metal strips, where 'L' is an equivalent inductance of the vertical dipoles, 'C' is the capacitance between the vertical ends of the two double-sided parallel crossed dipoles and the equivalent resistance 'R' corresponds to the ohmic losses of the metallic strips. The lumped element values of the equivalent circuit are commonly calculated using (1), (6), and (8), where 'P', 'l', 'w', and 'g' are the dimensions of the unit cell of a double-sided parallel crossed-dipole respectively. The 'θ' is the incidence angle with the normal incidence.

The equivalent inductance 'L' is given by Marcuvitz [12] as

$$\omega L = Z_0 \frac{l}{P} \cos\theta F\,(P, w, \lambda_0, \theta) \tag{1}$$

where 'ω' is an angular frequency, Z_0 and λ_0 are free-space wave impedance, and wavelength respectively, and (2) and (3), as shown at the bottom of the next page,
where,

$$A_{\pm} = \frac{1}{\sqrt{\left[1 \pm \frac{2P\sin\theta}{\lambda_0}\right] - \left(\frac{P\cos\theta}{\lambda_0}\right)^2}} - 1 \tag{4}$$

$$\beta = \sin\left(\frac{\pi s}{2P}\right), \quad \text{with } s = w \text{ or } g \tag{5}$$

The equivalent capacitance 'C' is given by Langley and Drinkwater [15] as

$$\omega C = 4Y_0 \frac{(2 \times w + g)}{P} \cos\theta F\,(P, g, \lambda_0, \theta)\,\varepsilon_{eff} \tag{6}$$

where ''ω' is the angular frequency, Y_0 and λ_0 are free-space wave admittance and wavelength, respectively.

The factor ε_{eff} in (6) represents an effective permittivity [14] and is calculated by

$$\epsilon_{eff} = \epsilon_{rh} + (\epsilon_{rh} - 1)\left[\frac{-1}{exp^N\,(x)}\right] \tag{7}$$

with $x = (10^*h/P)$; where 'h' is the thickness of the substrate, 'P' is the size of the unit-cell, $\varepsilon_{\text{rh}} = \varepsilon_{\text{r}}$ (if dielectric presents on both sides of the FSS) and $\varepsilon_{\text{rh}} = (\varepsilon_{\text{r}} + 1)/2$ (if dielectric presents only on one side), and N is an exponential factor that varies from 1.3 to 1.8 for different cell shapes in terms of the unit-cell filling factor. For double-sided parallel cross-dipole-based FSS, the optimal value of 'N' is 1.3.

The equivalent resistance 'R' can be calculated from [16] as

$$R \approx R_s \frac{S}{A} \tag{8}$$

where 'Rs' is the surface resistance, $S = P^2$ is the area of one-unit-cell, and 'A' is the surface area of the lossy element within a single unit cell. Using Equations (1) to (8), the equivalent circuit parameters in Fig. 1(b) can be readily determined.

Finally, the quality factor Q of the proposed FSS can be derived by substituting (1), (2) and (8) in the quality factor expression ($Q = \sqrt{L}/R\sqrt{C}$) as

$$Q = \frac{Z_0 A}{2R_s S}\sqrt{\frac{l \times F\left(P, w, \lambda_0, \theta\right)}{(2 \times w + g) \times F\left(P, g, \lambda_0, \theta\right) \varepsilon_{eff}}} \tag{9}$$

From these formulas, it can be concluded that the Q factor is a function of the different geometric parameters of the unit cell. However, the values of the strip length and periodicity cannot be chosen freely. The dipole length is approximately equal to $\lambda/2$ at the resonance frequency, while the periodicity of the structure must be much smaller than the wavelength. Subsequently, the quality factor can be controlled freely by the strip width.

In summary, the synthesis procedure of the proposed FSS can be simplified as follows:

A. *First, with the given values of the center frequency (f_0) and quality factor (Q), the parameters of the equivalent circuit elements can be obtained.*
B. *The dipole length 'l' is approximately equal to $\lambda/2$ at the resonance frequency.*
C. *Based on this calculated dipole length 'l' and with a starting value of the metal width 'w', estimate the value of the FSS's periodicity using the relation of equivalent resistance i.e., Eq. (8).*
D. *By enforcing the angle of incidence at normal incidence and for a given substrate, determine the value of the metal width 'w' using Eq. (6).*

The above method allows the equivalent circuit shown in Fig. 1(b) to synthesize the desired filtering response. It demonstrates the relationship between the equivalent circuit elements and the physical dimensions of the proposed FSS.

III. NUMERICAL RESULTS

The synthesis steps described in Section II are followed to design a stop-band FSS having a resonant frequency at 10 GHz for an arbitrary value of quality factor $\boldsymbol{Q = 7.5}$. Hence, the values of EC parameters are calculated as R = 0.05 Ω, C = 0.031 pF, and L = 8 nH. After acquiring the equivalent circuit parameters and choosing the dielectric substrate (εr = 2.94, h = 0.13 mm, tan δ = 0.02), the initial values of the unit-cell dimensions are obtained. Hence, the dipole length 'l' = 11.1 mm, the element size (or the period of the unit cell) 'P' = 11.6 mm, and the dipole strip width 'w' = 0.2 mm. It should mention that these physical parameters are obtained for the normal incidence. Based on these values, the proposed FSS is designed, and verified with the full-wave simulation. The obtained geometrical parameters of the unit-cell are tuned by using Ansys HFSS [17] to reach the desired frequency response. The transmission coefficient predicted by the equivalent circuit model is compared with the simulated results obtained by the initial geometry parameters and the tuned parameters are shown in Fig. 2. It is observed that the optimized HFSS simulated results are in close agreement with the obtained theoretical results. The surface current distribution of the proposed FSS for TE and TM modes is depicted in Fig. 3. From this figure, it is evident that the proposed model has the same frequency response for both modes.

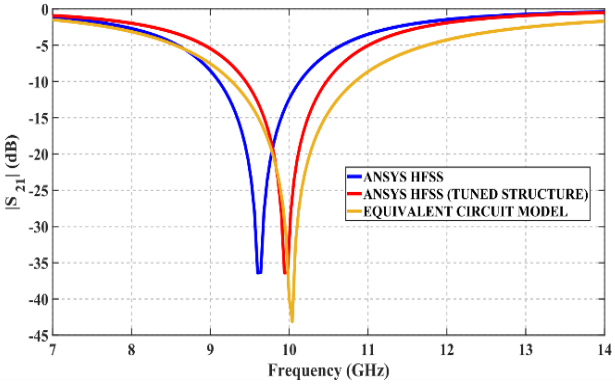

FIGURE 2. Transmission coefficient obtained by different methods for normal incidence.

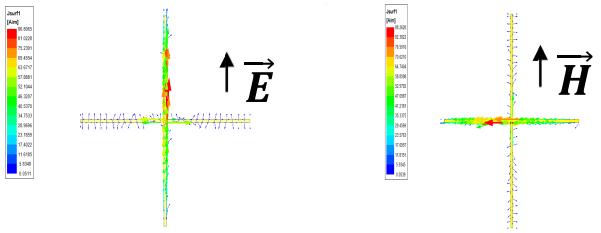

FIGURE 3. Surface current distribution of the proposed FSS at 10 GHz. (a) TE, and (b) TM mode of polarization.

IV. BANDWIDTH ENHANCEMENT

To obtain a wide stopband, the quality factor (Q) has to be decreased. Based on the filter theory [13], Q can be reduced by reducing the equivalent inductance and increasing the equivalent capacitance at the same time. From Eq. (1) described in section II, it is evident that using a large value of inductive element implies a gradual shift of the resonance

$$F\left(P, s, \lambda_0, \theta\right) = \frac{P}{\lambda_0}\left[\ln\left\{\frac{\csc \pi s}{2P}\right\}\right] + G\left(P, s, \lambda_0, \theta\right) \tag{2}$$

$$G\left(P, s, \lambda_0, \theta\right) = \frac{(1-\beta)^2\left[\left(1-\beta^2/4\right)\left(A_+ + A_-\right) + 4\beta^2 A_+ A_-\right]}{2 \times \left(1-\beta^2/4\right) + \beta^2\left(1+\beta^2/4-\beta^2/4\right)\left(A_+ + A_-\right) + 2\beta^6 A_+ A_-} \tag{3}$$

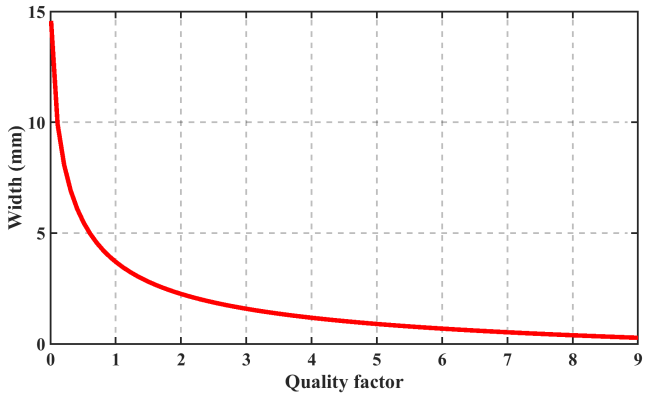

FIGURE 4. Plot for strip-width (w) as a function of the quality factor.

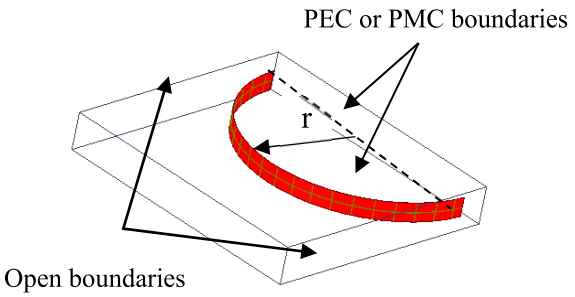

FIGURE 5. Simulation setup of the conformal FSS.

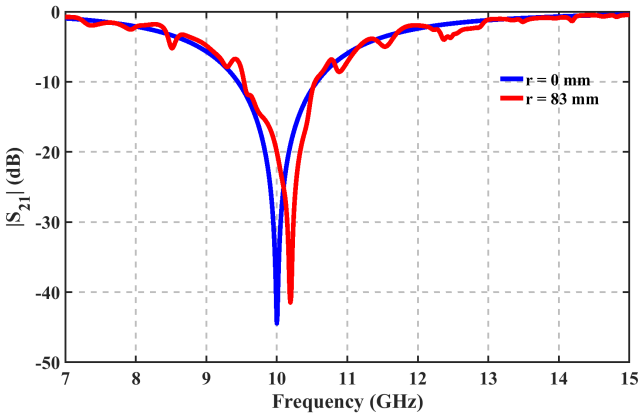

(a)

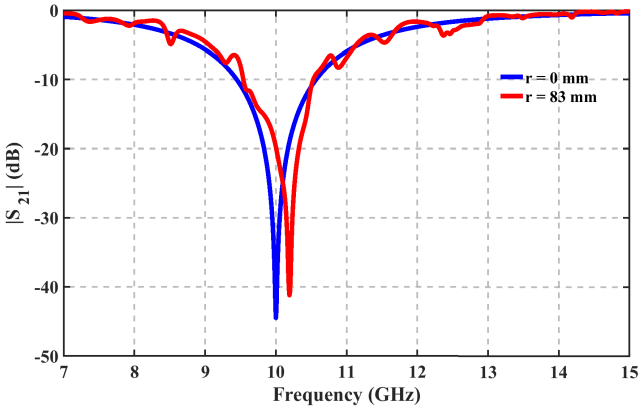

(b)

FIGURE 6. Simulated transmission coefficient for conformal and planar FSS at normal incidence (a) TE, and (TM) modes respectively.

frequency and generates poor stability under oblique incidence. Therefore, it is necessary to keep the inductance constant and, at the same time, increase the capacitance of the FSS to obtain a larger bandwidth. From Eq. (6) described in section II, it is necessary to choose a wider element to increase the capacitance of the FSS. For this reason, the metal width of the unit-cell is predicted as a function of the quality factor Q. Based on Eq. (9), the value of the metal width can be estimated for various values of Q. By using this synthesis method, the dipole width of the unit-cell is estimated for given frequency response and dielectric substrate at normal incidence. The data used for this case is as follows: the resonant frequency is 10 GHz, and the FSS is designed on a 0.13 mm thick RT/Duroid 6002 substrate with a relative dielectric constant of 2.94. The illustrated Fig.4 represents the strip width 'w' of the unit-cell under the quality factor variation. It can be observed that, for a wider bandwidth performance, should use a wider metal strip.

V. CONFORMAL BEHAVIOUR

In real-time applications, such as aerospace fuselage, parabolic reflectors, radome antennas, and many others, the conformal FSS has a significance, which is flesh mounted to the surface. Hence, the conformal behavior of the proposed FSS is analyzed using the bending option in Ansys HFSS. Based on a semi-infinite model described in [18], the conformal FSS is evaluated, and the same is simulated, as shown in Fig. 5. A finite array of FSS with 1×25 is simulated using wave ports. The top and bottom walls of the waveguide are assigned as PEC or PMC boundaries, whereas the side walls are assigned as open boundaries. This technique helps to evaluate the conformal structure at normal incidence. Fig. 6 shows the simulated transmission coefficient for planar and conformal FSS. It should also mention that the frequency response of the planar geometry is obtained by using periodic boundary conditions.

Fig. 6 presents the comparison of the simulated transmission coefficient of the conformal FSS and the planar FSS at the normal angle of incidence for both polarizations. It is observed that the resonant frequency for the FSS shifts from 10 GHz when the structures are bent. Fig. 6(a) shows that for the TE mode of polarization at the normal incidence, when the FSS is bent with a radius (r) of 83 mm, the simulated resonance frequency is shifted from 10 GHz to 10.19 GHz. On the other hand, for the TM mode of polarization, as shown in Fig. 6(b), the resonance frequency is shifted from 10 GHz to 10.2 GHz. This slight variation in the resonance frequency for both the polarization is attributed to the variation of the impedance proprieties and the interelement coupling of the FSS when it is bent [19].

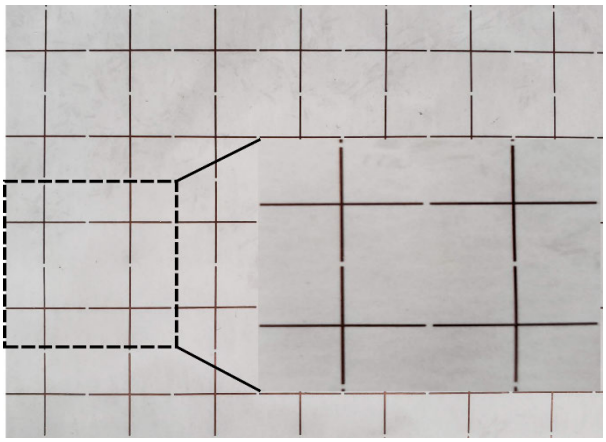

FIGURE 7. Photograph of the fabricated FSS prototype.

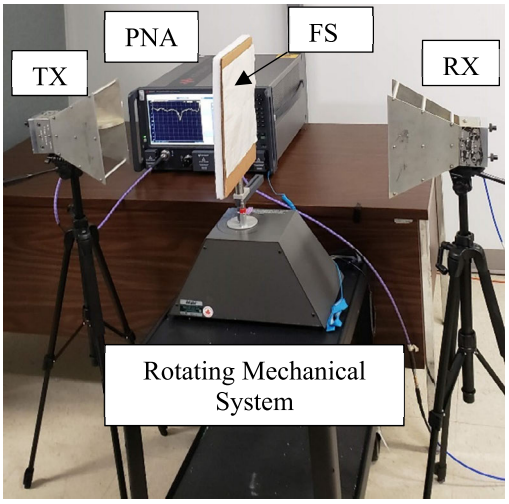

(a)

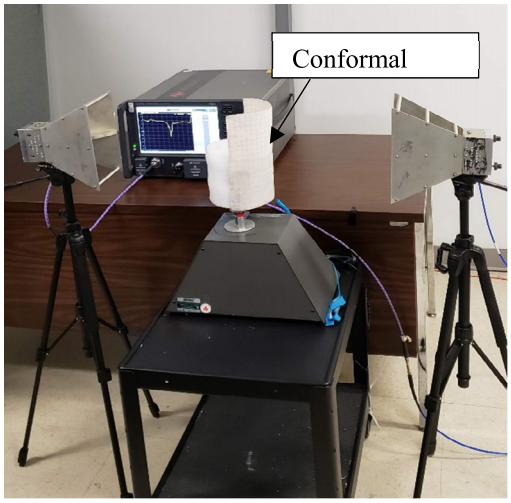

(b)

FIGURE 8. Experimental setup for measuring transmission coefficient for (a) Planar and (b) Conformal FSS.

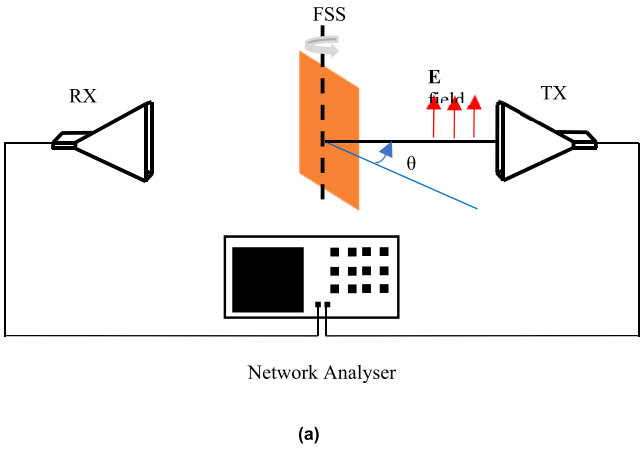

(a)

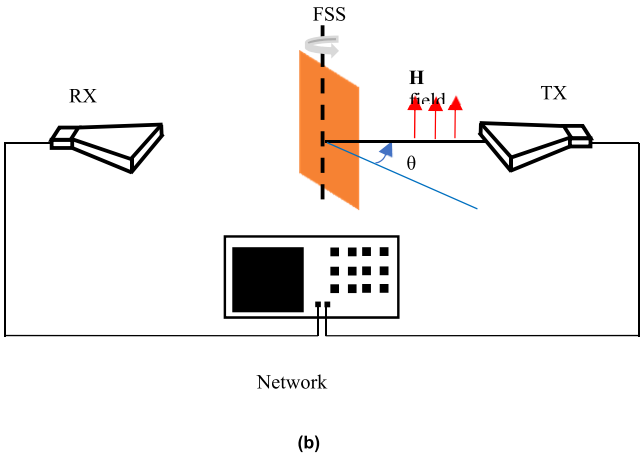

(b)

FIGURE 9. Measurement method for (a) TE, and (b) TM mode of polarization.

VI. EXPERIMENTAL RESULTS

A. PLANAR FSS

To experimentally validate the synthesis method described in section II, a prototype of the double-sided parallel cross-dipoles FSS, as shown in Fig. 7, is fabricated and measured. The dimensions of the FSS prototype are 304 mm × 304 mm, containing 25 × 25 elements for a metal width of 0.2 mm, a dipole length of 11.91 mm, and a periodicity of 12.16 mm, respectively. The measurement is performed in an enclosed room, where two wideband horns (1 GHz to 18 GHz) are used in the experimental setup. As shown in Fig. 8, the FSS prototype is placed between horn antennas, and the measurements are taken using an Agilent (PNA-X N5242A) network analyzer. As a reference, the transmission coefficient without FSS structure is measured. After that, the subsequent measurements of the transmission coefficients, for various angles of incidence and polarization, are obtained using a rotating mechanical system. The TE and TM modes were measured by using the method described in Fig. 9.

The measured transmission coefficient for both TE and TM mode of polarizations for various angles of incidence are plotted in Fig. 10. The measured FSS response for the TE polarization with different angles of incidence is plotted in Fig. 10(a). For the TE mode of polarization, it is observed that, as the angle of incidence increases, the bandwidth

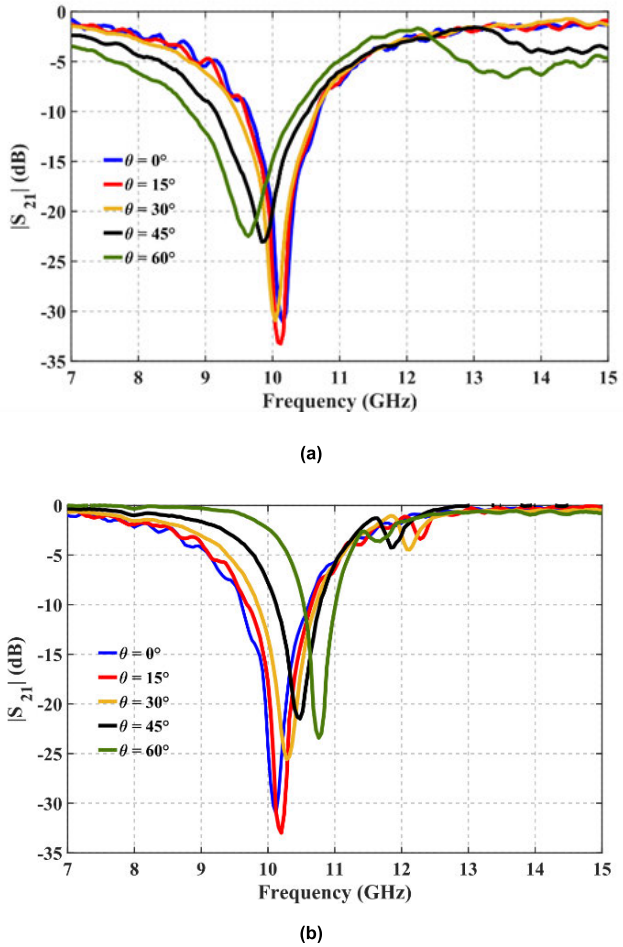

FIGURE 10. Measured transmittance for (a) TE, and (b) TM mode of polarization.

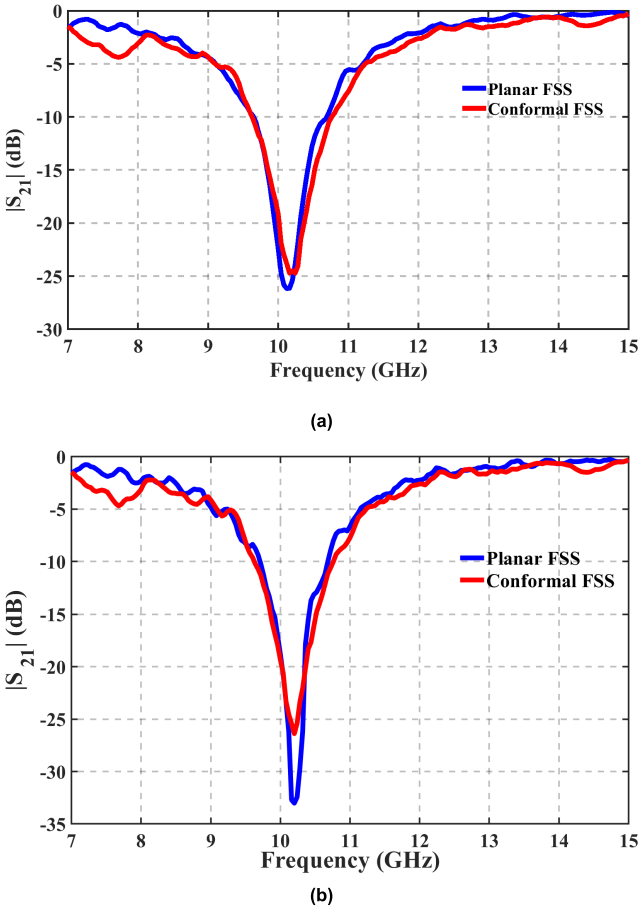

FIGURE 11. Measured transmission coefficient for conformal and planar FSS at normal incidence (a) TE, and (TM) modes respectively.

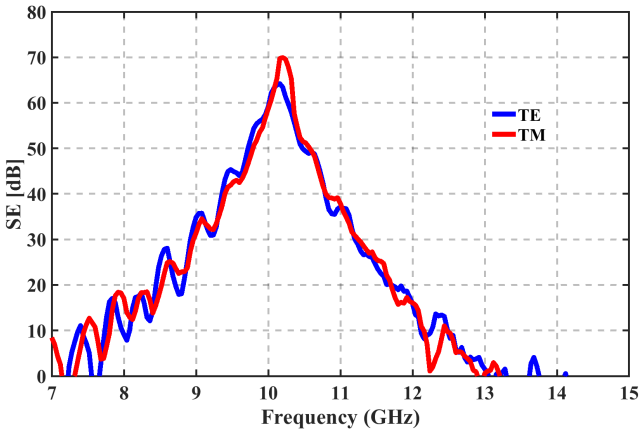

FIGURE 12. Measured shielding effectiveness of the proposed FSS for both polarizations at normal incidence.

increases. Different behavior is observed for TM mode of polarization as shown in Fig. 10(b), when the angle of incidence increases from 0° to 60°, the bandwidth decreases. The resonant frequency shift is observed for both polarizations when the incident wave angle varies from 0° to 60°. This occurs due to the impedance on the angle of incidence as given by the relation ($Z_{TE} = Z_0/\cos\theta, Z_{TM} = Z_0 * \cos\theta$).

B. CONFORMAL FSS

The transmission coefficient of the conformal FSS is obtained with a setup shown in Fig. 8(b) at normal incidence for both TE and TM modes. The planar FSS is bent on an arc of radius 'r' of 83 mm. The structure is attached to semi-circular cylinder foam that has similar dielectric properties with the free space ($\varepsilon_r = 1$). Fig. 11 shows the comparison of the measured transmission coefficient for both configurations. The conformal FSS exhibits a stable frequency response compared to the planar FSS at normal incidence for both polarizations.

To understand the shielding performance of the proposed FSS, shielding effectiveness (SE) is obtained using the equation (10):

$$SE\ (dB) = -20 \times \log \left| \frac{E_t}{E_i} \right| \tag{10}$$

Fig. 12 presents the shielding performance (SE) of the proposed FSS for both polarizations at normal incidence. It is evident that the proposed FSS provides a high SE level around

TABLE 1. Comparison with related works.

Ref	Element used	Center frequency (GHz)	Method	Flexibility	Number of layers
[11]	Complementary JC element	10	Analysis method	Yes	Single
[21]	Square loop	13.5	Synthesis method	No	Double
[22]	Crossed dipoles	8	Synthesis method	No	Single
[23]	Patch	10	Analysis	No	Single
Proposed work	Double-sided Crossed dipoles	10	Synthesis	Yes	Single

10 GHz for both TE and TM modes. Hence, the proposed FSS is suitable for EMI shielding applications.

Further, the comparison of the proposed work with the related works is shown in Table 1. It is evident from Table 1 that the proposed design method solves the synthesis problem, which is rarely described in the literature especially for double-sided crossed dipoles. The proposed synthesis method is based on the equivalent circuit model provides a simple way for designing conformal FSS, which can be applied in electromagnetic interference shielding applications. In addition, this method provides a formula for the Q factor as a function of the geometric parameters of the unit cell, which can be used to improve the bandwidth.

VII. CONCLUSION

In this paper, a simple method for synthesizing band-stop FSS and control of bandwidth is presented. The band-stop FSS consists of double-sided parallel cross-dipoles. The proposed conformal FSS is analyzed based on the equivalent circuit model at the desired frequency response, which allows acquiring the optimized physical parameters. The proposed work is verified by designing an ultra-thin FSS prototype having a band-stop response with a quality factor of 7.5 at 10 GHz. Full-wave simulations and experimental verifications have demonstrated the performance of the proposed FSS. The fabricated FSS is tested under different incident wave angles for both TE and TM modes of polarization.

ACKNOWLEDGMENT

The authors thank the valuable support and encouragement of the National Sciences and Engineering Research Council of Canada (NSERC) in executing the project.

REFERENCES

[1] A. Petosa, "Engineering the 5G environment," in *Proc. IEEE 5G World Forum (5GWF)*, Silicon Valley, CA, USA, Jul. 2018, pp. 478–481, doi: 10.1109/5GWF.2018.8516930.

[2] S. Raut and A. Petosa, "Engineering the environment to enhance millimetre-wave communications for connected vehicles," in *Proc. 48th Eur. Microw. Conf. (EuMC)*, Madrid, Spain, Sep. 2018, pp. 304–307, doi: 10.23919/EuMC.2018.8541394.

[3] C. Liaskos, S. Nie, A. Tsioliaridou, A. Pitsillides, S. Ioannidis, and I. Akyildiz, "A new wireless communication paradigm through software-controlled metasurfaces," *IEEE Commun. Mag.*, vol. 56, no. 9, pp. 162–169, Sep. 2018, doi: 10.1109/MCOM.2018.1700659.

[4] A. Petosa, N. Gagnon, C. Amaya, M. Li, S. Raut, J. Ethier, and R. Chaharmir, "Characterization and enhancement of the environment for 5G millimetre-wave broadband mobile communications," in *Proc. 12th Eur. Conf. Antennas Propag. (EuCAP)*, London, U.K., Apr. 2018, pp. 1–5, doi: 10.1049/cp.2018.0710.

[5] B. Lin, S. Liu, and N. Yuan, "Analysis of frequency selective surfaces on electrically and magnetically anisotropic substrates," *IEEE Trans. Antennas Propag.*, vol. 54, no. 2, pp. 674–680, Feb. 2006, doi: 10.1109/TAP.2005.863136.

[6] V. P. Silva Neto, A. G. D'Assuncao, and H. Baudrand, "Analysis of finite size nonuniform stable and multiband FSS using a generalization of the WCIP method," *IEEE Trans. Electromagn. Compat.*, vol. 60, no. 6, pp. 1802–1810, Dec. 2018, doi: 10.1109/TEMC.2017.2785787.

[7] F. Costa, A. Monorchio, and G. Manara, "An equivalent circuit model of frequency selective surfaces embedded within dielectric layers," in *Proc. IEEE Antennas Propag. Soc. Int. Symp.*, North Charleston, SC, USA, Jun. 2009, pp. 1–4, doi: 10.1109/APS.2009.5171774.

[8] S. Ghosh and K. V. Srivastava, "An equivalent circuit model of FSS-based metamaterial absorber using coupled line theory," *IEEE Antennas Wireless Propag. Lett.*, vol. 14, pp. 511–514, 2015, doi: 10.1109/LAWP.2014.2369732.

[9] D. Li, T.-W. Li, R. Hao, H.-S. Chen, W.-Y. Yin, H.-C. Yu, and E.-P. Li, "A low-profile broadband bandpass frequency selective surface with two rapid band edges for 5G near-field applications," *IEEE Trans. Electromagn. Compat.*, vol. 59, no. 2, pp. 670–676, Apr. 2017, doi: 10.1109/TEMC.2016.2634279.

[10] P.-C. Zhao, Z.-Y. Zong, W. Wu, B. Li, and D.-G. Fang, "Miniaturized-element bandpass FSS by loading capacitive structures," *IEEE Trans. Antennas Propag.*, vol. 67, no. 5, pp. 3539–3544, May 2019, doi: 10.1109/TAP.2019.2902633.

[11] V. Krushna Kanth and S. Raghavan, "Design and optimization of complementary frequency selective surface using equivalent circuit model for wideband EMI shielding," *J. Electromagn. Waves Appl.*, vol. 34, no. 1, pp. 51–69, Jan. 2020, doi: 10.1080/09205071.2019.1688691.

[12] N. Marcuvitz, *Waveguide Handbook*. New York, NY, USA: McGraw-Hill, 1951.

[13] K. L. Kaiser, *Electromagnetic Compatibility Handbook*. Boca Raton, FL, USA: CRC Press, 2005.

[14] A. I. Zverev, *Handbook of Filter Synthesis*. Hoboken, NJ, USA: Wiley, 1967.

[15] R. J. Langley and A. J. Drinkwater, "Improved empirical model for the Jerusalem cross," *IEE Proc. H-Microw., Opt. Antennas*, vol. 129, no. 1, pp. 1–6, Feb. 1982, doi: 10.1049/ip-h-1.1982.0001.

[16] F. Costa, A. Monorchio, and G. Manara, "Efficient analysis of frequency-selective surfaces by a simple equivalent-circuit model," *IEEE Antennas Propag. Mag.*, vol. 54, no. 4, pp. 35–48, Aug. 2012, doi: 10.1109/MAP.2012.6309153.

[17] *ANSYS HFSS Version 2018.0.0*. [Online]. Available: https://www.ansys.com

[18] M. Nauman, R. Saleem, A. K. Rashid, and M. F. Shafique, "A miniaturized flexible frequency selective surface for X-band applications," *IEEE Trans. Electromagn. Compat.*, vol. 58, no. 2, pp. 419–428, Apr. 2016, doi: 10.1109/TEMC.2015.2508503.

[19] R. C. Rumpf, M. Gates, C. Kozikowski, and W. A. Davis, "Guided-mode resonance filter compensated to operate on a curved surface," *Prog. Electromagn. Res. C*, vol. 40, pp. 93–104, Jun. 2013, doi: 10.2528/PIERC13041209.

[20] I. S. Syed, Y. Ranga, L. Matekovits, K. P. Esselle, and S. G. Hay, "A single-layer frequency-selective surface for ultrawideband electromagnetic shielding," *IEEE Trans. Electromagn. Compat.*, vol. 56, no. 6, pp. 1404–1411, Dec. 2014, doi: 10.1109/TEMC.2014.2316288.

[21] N. Liu, X. Sheng, C. Zhang, J. Fan, and D. Guo, "A design method for synthesizing wideband band-stop FSS via its equivalent circuit model," *IEEE Antennas Wireless Propag. Lett.*, vol. 16, pp. 2721–2725, 2017, doi: 10.1109/LAWP.2017.2743114.

[22] R. M. S. Cruz, P. H. da F. Silva, and A. G. D'Assuncao, "Synthesis of crossed dipole frequency selective surfaces using genetic algorithms and artificial neural networks," in *Proc. Int. Joint Conf. Neural Netw.*, Jun. 2009, pp. 627–633, doi: 10.1109/IJCNN.2009.5178927.

[23] P. H. da F. Silva, R. M. S. Cruz, and A. G. d'Assuncao, "Blending PSO and ANN for optimal design of FSS filters with koch island patch elements," *IEEE Trans. Magn.*, vol. 46, no. 8, pp. 3010–3013, Aug. 2010, doi: 10.1109/TMAG.2010.2044147.

YASSINE ZOUAOUI was born in Tunis, Tunisia, in 1989. He received the B.A.Sc. degree in information and communication technologies from the University of El Manar, Tunis, in 2011, and the M.Sc. degree in electronic, electrotechnical and automatic (EEA), in 2014. He is currently pursuing the Ph.D. degree with the Department of Computer Science and Engineering, University of Quebec in Outaouais, Gatineau, QC, Canada. His current research interests include fundamental electromagnetic theory, periodic structures, antennas, and microwave circuits.

LARBI TALBI (Senior Member, IEEE) received the M.S. and Ph.D. degrees in electrical engineering from Laval University, Quebec City, QC, Canada, in 1989 and 1994, respectively.

From 1994 to 1995, he was a Postdoctoral Fellow with the Personal Communications Research Group, INRS Telecommunications, Montreal, QC, Canada, where he led projects supported by Bell Canada. From 1995 to 1998, he was an Assistant Professor with the Electronics Engineering Department, Riyadh College of Technology, Saudi Arabia. From 1998 to 1999, he was an Invited Professor with the Electrical and Computer Engineering Department, Laval University. He joined the Department of Computer Science and Engineering (DCSE), University of Quebec in Outaouais (UQO), Gatineau, QC, Canada, as a Professor, in 1999. He spent his sabbatical leave as an Invited Researcher with the Communication Research Center, Ottawa, ON, Canada, within the Propagation Research (RVEP) Group, Satellite Communications and Radio Propagation Branch (VPSAT), in 2005. He joined the Electrical and Electronics Engineering Department, Dumlupinar University, Turkey, as a Visiting Professor, in 2006. From 2007 to 2013, he was the Ph.D. Program Chair in sciences and information technologies and the Chair of the department, from 2013 to 2015. He has a very strong collaboration with the Telebec Wireless Underground Communication Laboratory, Val-d'Or, QC, Canada. He is currently a Full Professor with the DCSE, UQO. He has authored or coauthored over 200 journal articles and conference technical papers. His research interests include experimental characterization and modeling of UHF/extremely high-frequency indoor radio propagation channels and design of antennas and microwave circuits for wireless communication systems. He is currently actively involved in major projects related to the deployment of wireless technologies in underground mines, mainly, the experimental characterization of the underground mine channels using multi-in multi-out antennas at 60 GHz, the design of microwave and RF components using substrate integrated waveguide technique, transparent antennas, metamaterials applied to microwave design, and antenna array for wireless applications. He received the Best Paper Prize from the IET—ICWCA Conference, Malaysia, in 2013. He is a member of the Order of Engineers of Quebec. He frequently serves as a technical program committee member for international and national conferences. He is an Associate Editor of the *International Journal of Antennas and Propagation* (Hindawi Publishing Corporation). He regularly acts as a reviewer for many international scientific journals and conferences and also for research funding organizations.

KHELIFA HETTAK (Senior Member, IEEE) received the Dipl.Ing. degree in telecommunications from the University of Algiers, Algeria, in 1990, and the M.A.Sc. and Ph.D. degrees in signal processing and telecommunications from the University of Rennes 1, France, in 1992 and 1996, respectively.

Since January 1997, he has been with the Personal Communications Staff of INRS Télécommunications, where he was involved. He has been an Associate Researcher with the Electrical Engineering Department, Laval University, since October 1998, where he was involved in RF aspects of smart antennas. Since August 1999, he has been with the Terrestrial Wireless Systems Branch, Communications Research Centre (CRC), Ottawa, ON, Canada, as a Research Scientist. He was involved in developing MMICs at 60 GHz, low temperature cofired ceramic (LTCC) packaging, RF MEMS switches, and GaN robust Tx/Rx modules. He is actively involved in microwave/millimeter-wave systems and related front-end analog electronic circuits, phased arrays, and satellite communication systems. He also is active in planar antenna design including wide scan-angle antennas at 60 GHz for wireless applications. He recently started an effort in CMOS/SiGe RFIC design for the 60 GHz region, with the particular emphasis on developing miniature phase shifters using CMOS/SiGe technology for phased-array applications, oscillators, and switches for millimeter-wave communication systems (OSA).

NARESH K. DARIMIREDDY (Senior Member, IEEE) received the B.Tech. degree in ECE from S. V. University, the M.E. degree (EC) from UVCE (A), Bangalore University, the M.B.A. degree from Central University Pondicherry, and the Ph.D. degree from UCEK (A), JNTU, Kakinada. He is currently a Postdoctoral Fellow with the Université du Québec à Rimouski (UQAR), Rimouski, QC, Canada, and the fellowship is awarded by PBEEE-FRQNT, Government of Quebec. He was awarded as the Best Researcher for the year 2018–2019 from JNT University, Kakinada. He has 15 years of industry and teaching experience. He had published 53 technical journals and conferences of repute and four patents (India). His research interests include microwave antennas, planar antennas, dielectric antennas, metamaterials, filters, and couplers. He is a Senior Member of the IEEE (A & P Society) and IE (I).